Nano-array Integrated Monolithic Devices: Toward Rational Materials Design and Multi-Functional Performance by Scalable Nanostructures Assembly

Sibo Wang, Zheng Ren, Yanbing Guo, and Pu-Xian Gao*
Nanomaterials Science Laboratory, Department of Materials Science and Engineering & Institute of Materials Science, University of Connecticut, Storrs, CT 06269-3136, USA
*Email: puxian.gao@uconn.edu

Abstract

The scalable three-dimensional (3-D) integration of functional nanostructures into applicable platforms represents a promising technology to meet the ever-increasing demands of fabricating high performance devices featuring cost-effectiveness, structural sophistication and multi-functional enabling. Such an integration process generally involves a diverse array of nanostructural entities (nano-entities) consisting of dissimilar nanoscale building blocks such as nanoparticles, nanowires, and nanofilms made of metals, ceramics, or polymers. Various synthetic strategies and integration methods have enabled the successful assembly of both structurally and functionally tailored nano-arrays into a unique class of monolithic devices. The performance of nano-array based monolithic devices is dictated by a few important factors such as materials substrate selection, nanostructure composition and nano-architecture geometry. Therefore, the rational material selection and nano-entity manipulation during the nano-array integration process, aiming to exploit the advantageous characteristics of nanostructures and their ensembles, are critical steps towards bridging the design of nanostructure integrated monolithic devices with various practical applications. In this article, we highlight the latest research progress of the two-dimensional (2-D) and 3-D metal and metal oxide based nanostructural integrations into prototype devices applicable with ultrahigh efficiency, good robustness and improved functionality. Selective examples of nano-array integration, scalable nanomanufacturing and representative monolithic devices such as catalytic converters, sensors and batteries will be utilized as the connecting dots to display a roadmap from hierarchical nanostructural assembly to practical nanotechnology implications ranging from energy, environmental, to chemical and biotechnology areas.

Introduction

The increasingly severe energy shortage and environmental problems we are facing worldwide call for sustainable and renewable energy production, efficient energy utilization and environment protection. Amongst the various solutions, the design and exploration of new materials, devices and systems is one of the fundamental answers to meet these challenges. In the past few decades, the unique benefits discovered to be endowed by nanoscale materials have come along with extensive research and development of nanoscale devices and systems lately. By shrinking the component dimensions from macroscale down to nanoscale, the nanostructural entities are widely represented in the forms of 0-D nanodots and

nanoparticles, 1-D nanorods, nanowires and nanotubes, 2-D nanosheets and nanoplates. With the fast development of synthesis techniques, the ever-growing discoveries and improving understandings of new properties of nanostructures, nanotechnology has been tipped for a variety of applications in energy conversion and storage, exhaust emission control, environmental sensing and monitoring. For example, interesting electrical property was found on ultrafine single crystalline Bi nanowire with variable band structures due to the confinement of charge carriers transport along longitudinal direction.[1] Such band structure engineering enabled by low-dimension quantum confinement effect was also observed in metal oxide nanostructure array and plays an important role in photoelectrochemical applications [2,3] such as photo-oxidation of water. When tailored into 1-D nanostructures, metal oxide catalysts exhibit enhanced catalytic performance towards removal of toxic gases such as carbon monoxide and nitrogen monoxide,[4,5,6,7] which is strongly dependent upon the different activity from different crystal planes exposed. The CeO_2 nanorod was reported to be more reactive toward CO oxidation because of its predominantly exposed catalytically active crystal planes in {001} {110}.[8] In light of these unique physical and chemical properties, 1-D nanostructures have been employed as one of the most important building blocks for nanoscale device fabrication.[9] Used in light harvesting and energy storage devices, the electrodes assembled by 1-D metal oxide nanostructures with morphology control have been found to facilitate charge transport along axial direction, shorten the pathways for fast and sufficient ion diffusion with reduced internal resistance.[10,11,12,13,14]

Fast-forward to the 21st century, various nanostructural entities are being rationally assembled into microscale or even macroscale architectures in a well-defined hierarchical fashion. As an example, nanostructure array (nano-array) has become more and more important in meeting societal demands for nanotechnology. It not only presents a new grand challenge to bring the scientific discovery to realistic societal implications, but also builds up a usable platform collectively implemented by assembly of functional nanostructural components. These nanoscale architectural assemblies allow us fully utilizing their unique technological advantages such as metal-support interaction at interface,[15] fast electron transport properties in optoelectronics [16,17] and high surface area in environmental remediation.[18,19] The monolithic devices enabled by 1-D nanostructure assembly have been suggested to reduce the agglomeration of active sites, which improves the spatial utilization efficiency in a confined space. It thus offers greater chance of interaction between the active surface of nano-array and the target phases such as toxic gas and organic pollutant in a heterogeneous catalytic reaction [20,21,22,23] or electrolyte in energy conversion system.[24,25] From the industrial manufacturing perspective, the effective self-assembly of nano-array without usage of binders and involving multiple coating processes can provide a potentially promising route for cost-effective and scalable manufacturing.

On the other hand, the performance of nano-array integrated devices is intimately correlated with a variety of factors such as device substrate selection, nanostructure composition and dimensions, and geometrical distribution of nanoarchitecture(s). Therefore, to further improve the performance of monolithic nano-array devices with ultrahigh efficiency, long service lifetime and function diversity, the most adopted strategies in recent decades can be classified

into three categories: (1) proper screen and selection of material based on appropriate physical/chemical properties for optimized functions and performance; (2) combination of multiple material components to enable unexpected but enhanced functional performance and explore possible synergistic effects; (3) design of sophisticated hierarchical structures using either similar or dissimilar nanoscale building blocks of precisely controlled geometry and dimensionality to realize possible functionality optimization.

In this article, we present a comprehensive overview of the recent progress in nano-array integrated monolithic devices focusing on integration strategy, scalable manufacturing and device demonstration for nano-catalysis, energy storage and conversion as well as environmental sensing and monitoring. It is worth noting that although the presented examples have strong energy and environmental perspectives, this shall not limit the general applicability of the integrated nanomaterials design and device concepts highlighted here.

Nano-array integration strategy and manufacturing

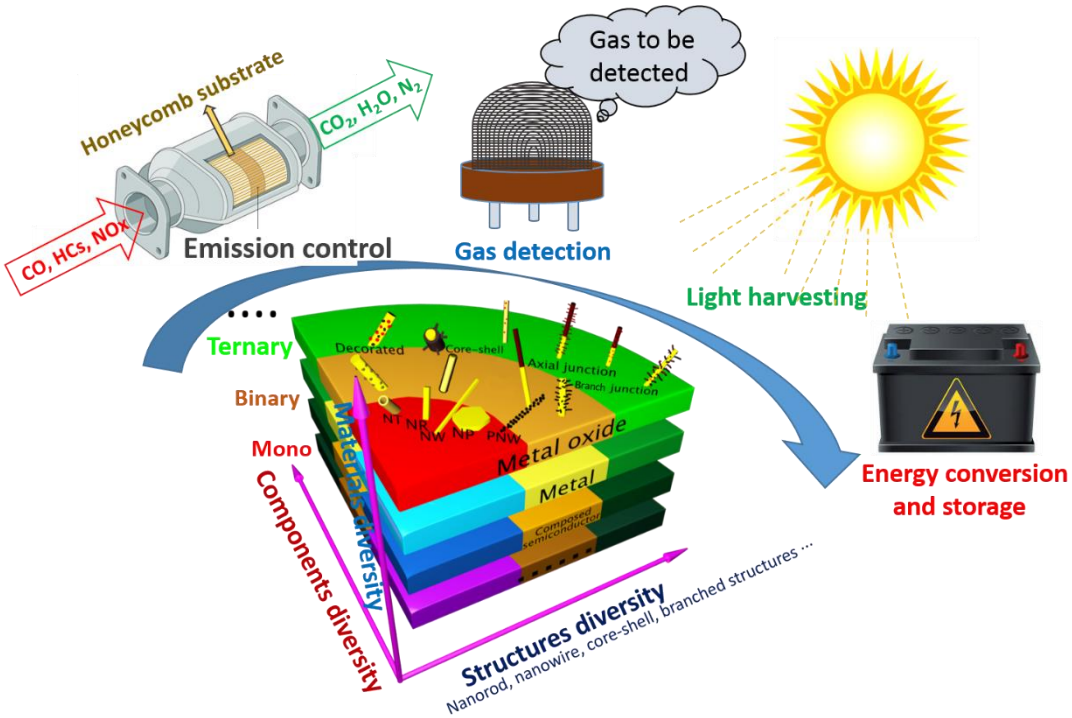

Figure 1 Platform of designing nano-array integrated devices and their energy and the environmental applications.

Nowadays, the versatile synthetic approaches of nano-array on various substrates provide an essential platform comprises a three-fold diversity in material, components and structures. This versatile diversity allows for design of high performance functional nano-array devices aiming at various environmental applications such as exhaust emission control, gas detection, light harvest and energy storage (Figure 1). Template-assisted synthesis [26] and traditional lithography process [27,28] are among the most effective approaches to prepare large-scale

nano-arrays with precisely controlled geometry and pattern on 2-D substrates. Compared with the relatively complicated fabrication procedures in top-down method, the wet chemical hydrothermal method represents a facile yet promising group of cost-effective strategies for large scale fabrication of nano-array based monolithic devices. Using hydrothermal method, 1-D nanorods, nanowires and nanotubes, and 2-D nanosheets and nanoplates can be assembled into array configuration on a variety of planar substrate.[29.30,31,32,33,34,35] One of the notable advantages of hydrothermal method is the feasibility of tunable nano-array geometry by parameter adjustment on temperature and concentration.

Meanwhile, the success in fabricating complicated yet well-controlled hierarchical nano-array structures have opened up new possibilities to enable combined and synergistic effects from either dissimilar material units or the hierarchical spatial arrangement. As shown in Figure 2 (a), a facile one-step synthesis has led to the evolution of anatase TiO_2 nanowire arrays from sparse distribution at initial growth stage to hierarchical forest array with densely packed nanorod braches interspacing the neighboring TiO_2 nanowires rooted on substrate.[36] Interestingly, even more complex hierarchical branched nano-array with multi-layered configuration can be constructed through a series of sequential hydrothermal growth based on preferentially induced growth mechanism (Figure 2 (b)).[37] Such branched nano-forest array represents a unique hierarchical nano-array configuration for the binary or ternary material components system. Recently, hydrothermal integration strategy has been adopted to integrate large-scale metal oxide nano-arrays on metal foam (Figure 2 (c)),[38] flexible carbon fiber paper and carbon cloth (Figure 2 (d)).[39] With the significantly enhanced electrical conductivity these substrates are able to provide, metal oxide nano-array integrated electrodes hold a great promise towards fabricating lightweight, flexible, and robust electronic devices.

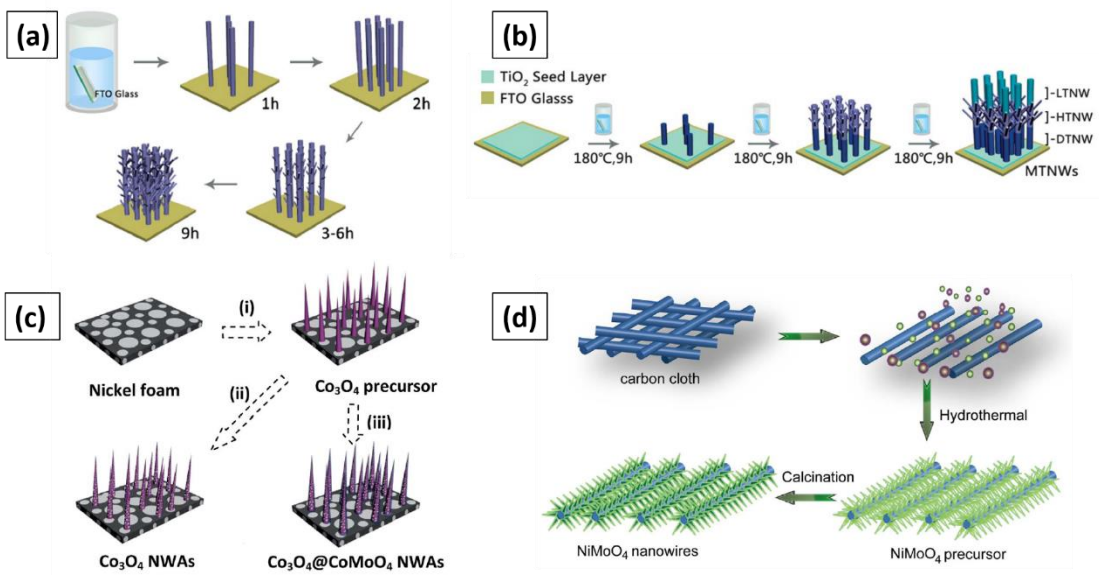

Figure 2 (a) Morphology evolution of hierarchical TiO_2 nano-array with increasing hydrothermal growth duration. Reproduced with permission from reference 36. (b) Formation of hierarchical TiO_2 nano-array by sequential multistep hydrothermal growth. Reproduced with permission from reference 37. (c) Co_3O_4 nanowire array and binary Co_3O_4@$CoMoO_4$ nanowire array on Ni foam substrate via (ⅰ) hydrothermal synthesis, (ⅱ) thermal treatment,

(iii) hydrothermal based ion exchange. Reproduced with permission from reference 38. (d) Illustration of $NiMoO_4$ nanowire array formation process on carbon cloth substrate. Reproduced with permission from reference 39.

Hierarchical nano-array could be achieved by assembling different constituents into defined framework. Core-shell nano-arrays consisting of 1-D nano-core, a typical nano-array architecture, can be assembled to selectively tailor the activity of target reactions by keeping the desired performance and suppressing unwanted ones. Various nano-shell deposition approaches including hydrothermal method have been used to control the nano-shell characteristics such as thickness, uniformity and grain size during the integration process in order to induce the desired functional performance. For example, the hydrothermal synthesis process combined with a pulse laser deposition (PLD) method was used to prepare large scale 2-D ZnO/(La, Sr)CoO_3 core-shell nanorods array (Figure 3 (a)) with good uniformity.[40] The ZnO/(La, Sr)CoO_3 core-shell nanorods array exhibited enhanced photocatalytic activity compared to their individual counterparts. It is worth pointing out that the nano-shell constituents are not limited to nanoparticles. Layered double hydroxide (LDH) nanoplatelets shell has been fabricated using electrochemical deposition upon hydrothermally grown transition-metal-oxide nanorod arrays (Figure 3 (b)).[41] The LDH nano-shell is uniformly anchored on the surface of nano-array while the thickness and morphology are precisely controlled by electrodeposition duration. Such combination of different synthetic approaches enables design of sophisticated nanoarchitectures with well-designed subunits, giving rise to well-defined nano-array integrated electrodes.

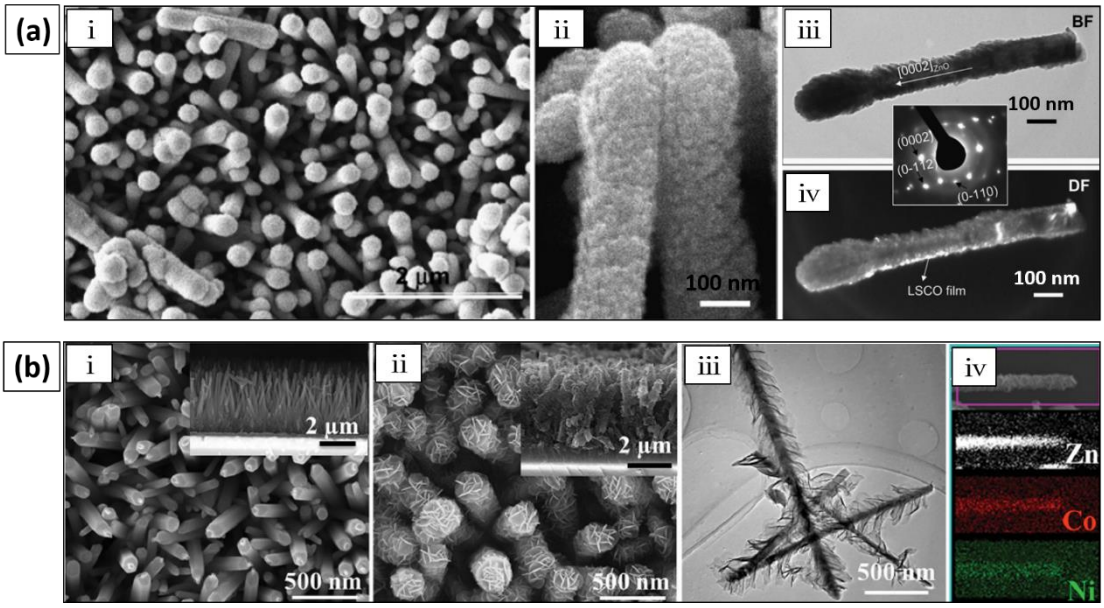

Figure 3 (a) (ⅰ)Top view and (ii) cross-sectional view SEM images composite core-shell nanorod arrays comprised of hydrothermal grown ZnO nanorods and pulse laser deposited LSCO nanofilm; (iii) bright field and (iv) dark field TEM images and corresponding electron diffraction pattern of individual ZnO/LSCO composite core-shell nanorod. Reproduced with permission from reference 40. (b) (ⅰ)SEM image of ZnO nanowire array on FTO substrate achieved by hydrothermal synthesis; (ii) ZnO@LDH core-shell nanowire array fabricated by

electrochemical deposition; (iii) TEM image and (iv) EDX mapping of ZnO@CoNi-LDH nanowires. Reproduced with permission from reference 41.

Recently, three-dimensional (3-D) integration of nanostructure arrays (nano-arrays) in multi-channeled monolithic substrates has been studied to translate the unique properties of nano-arrays from 2-D planar platforms into 3-D configurations. However, the direct integration or in-situ growth of 1-D nano-arrays inside 3-D configurated substrates is a nontrivial task due to usually insufficient mass transport in geometry-confined spaces in either microscale or millimeter scale leading to nonuniform distribution of nano-arrays. In this case, three states of mass have been investigated. For example, Wang and coworkers reported a surface-reaction-limited pulsed chemical vapor deposition (SPCVD) technique to build large-scale TiO_2 nanorod array in space-confined channels by taking advantage of good diffusion of gaseous precursors and anisotropic crystal growth habit (Figure 4 (a)).[42] Meanwhile, wet chemical approaches involving solution precursors are usually favored by industrial manufacturing of monolithic devices due to relatively low cost and scale-up feasibility. Gao and coworkers developed a green and convenient hydrothermal approach to integrate commercial honeycomb substrate with a series of transition metal oxide (TMO) 1-D nano-array (Figure 4 (b)).[43] By using different metal salt precursors and tuning the growth conditions, ZnO nanorod array, TiO_2 nanorod array, CeO_2 nanotube array, and Co_3O_4 nanowire array can be cost-effectively integrated on the wall surface featuring impressive high surface area, thermal stability and mechanical robustness. The 3-D hydrothermal integration strategy is able to manipulate nano-array's size, shape, structure and thus an improved gas-solid phase interaction and tailored multifunctional catalytic performance towards exhaust emission control.

The ability of building structural complex with atomic precision defines the feature of nano-array technology. For some metal oxides, e.g. perovskite-type materials, 3-D nano-array structures have been mostly constructed with the assistance of templates.[44] A facile sonication assisted wash-coating method was further demonstrated recently by Gao and coworkers to integrate 3-D ZnO nanorod array with a uniformly dispersed coating composed of perovskite-type metal oxide nanoparticles (Figure 4(c)).[45] The heterogeneous nano-interfaces in the core-shell nano-arrays and good dispersion of perovskite nanoparticles give rise to enhanced catalytic performance towards propane oxidation at low temperature. The novel integration strategy of 1-D metal oxide nano-array in monolithic honeycomb substrate represents a milestone for developing practical nanomanufacturing of 3-D nano-array integrated monolithic devices.

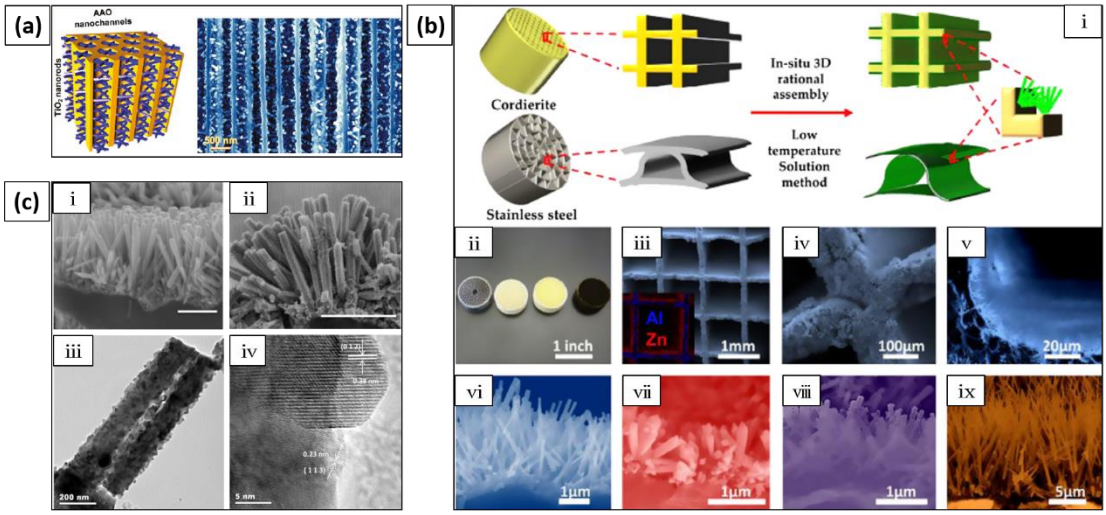

Figure 4 (a) Schematic illustration and SEM image of TiO_2 nanorod arrays in space confined channels of AAO substrate. Reproduced with permission from reference 42. (b) (i) Schematic nano-array assembly process on typical 3-D cordierite and stainless steel monoliths via hydrothermal synthesis; (ii) Photographs of various metal oxide nano-array deposited monolith catalysts; (iii) low magnification SEM image of ZnO nano-array catalysts with element distribution; (iv) and (v) low magnification SEM image of nano-array rooted on the channel wall cross-section; (vi)-(ix) side view of ZnO nanorod array, TiO_2 nanorod array, CeO_2 nanotube array and Co_3O_4 nanowire array. Reproduced with permission from reference 43. (c) (i) and (ii) cross-sectional view of ZnO nanorod and ZnO/$LaCoO_3$ core-shell nanorod arrays rooted on wall surface of cordierite substrate; (iii) bright field TEM image of ZnO/$LaCoO_3$ core-shell nanorod; (iv) high resolution TEM image showing crystalline perovskite-type $LaCoO_3$ nanoparticles on the surface of ZnO. Reproduced with permission from reference 45.

New principles in the scalable nanostructure assembly

The thriving nanostructures design methodology and demonstrated functional performance require compatible large scale integration strategy, which plays an essential role to bridge laboratory-scale nano-device with industrially relevant nanomanufacturing. Therefore, synthetic strategies compatible to various types of substrates and material species are highly desired for large-scale self-assembly of nano-array devices. Zhang and coworkers reported an intriguing chemical bath deposition method to produce a wide spectrum of TMO nano-array based electrodes. Combined proper calcination process, this facile and general integration strategy features simplified operation, low reaction temperature and pressure, and feasibility for a variety of binary and ternary hierarchical branched and core-shell mesoporous nano-arrays on various conductive 2-D flat substrates and 3-D porous metal foam (Figure 5 (a)).[46] Fast integration, as another important prerequisite for industrially-relevant scalable self-assembly of nano-array devices, requires the pursuit of substitutive growth mechanism and heating source that can essentially enhance the reaction rate. For instance, impurity-free and high surface-to-volume ratio ZnO nanorod array on 2-D substrate can be rapidly prepared

via the reaction of zinc acetate dehydrate in aged ethylenediamine (EDA) (Figure 5 (b)) [47,48], which is distinct from conventional reaction mechanism of ZnO nanorod hydrothermal growth.

In the past few years, microwave irradiation assisted crystal growth is emerging as a promising strategy for large-scale production of nanostructures. Significant amount of literature has been documented in the microwave synthesis of freestanding nanoparticles, which usually are characterized as a result of homogeneous nucleation and growth in aqueous solutions.[49,50,51,52,53,54] And there are some nice reviews that have systematically introduced the benefits provided by microwave heating in preparation of nanostructures via solvothermal methods, such as the accelerated heating rate and reaction rate compared to conventional heating source.[55,56] In contrast, nano-array assemblies via microwave irradiation call for boosted heterogeneous growth and control of nanostructure orientation, which are usually negligible in the synthesis of free-standing nanoparticles. Due to the broad application potential of ZnO nano-array devices, lately an increasing amount of studies has been conducted on microwave assisted hydrothermal synthesis of ZnO nano-arrays on planar substrates in which the growth duration can be significantly reduced.[57,58,59] For example, using microwave heating in a typical continuous flow synthesis of ZnO nanowire arrays, the synthetic duration can be reduced by 6 times compared to conventional heating scenario, while achieving comparable ZnO nanowire array on flat substrates.[60,61] It is worth noting that although continuously injected fresh solution favors the dynamic equilibrium of solution concentration, the homogeneous nucleation and particle growth is still dominant under microwave irradiation, leading to significantly compromised nano-array growth rate and precursor utilization efficiency. Therefore, controllable preferential growth of nano-array at targeted location has become another challenge for developing fast integration strategy. Recently, laser induced hydrothermal growth (LIHG) was reported as one-step synthesis approach of ZnO nanowire arrays. It enables rapid and controlled growth at selective area by using digital scanning of focused laser beam, which provides localized heating source and greatly simplifies the growth process.[62]

From the perspective of sustainable chemistry, the environmentally benign assemblies with low energy consumption are favorable for scalable manufacturing of nano-devices. Hydrothermal based integration has shown its capability of constructing 3-D nano-array integrated monolithic catalysts, however, challenges remain on the way of scaling up substrate's dimensionality owing to the poor mass transport and nonuniformity of nano-array across space-confined channels. Mechanical agitation of oscillating stirring has been proved to be an effective approach to promote the precursor replenishment and induce a relatively uniformly distributed nano-array in elongated channels. Meanwhile, the synthetic duration and material utilization, also known as important figure of merits in industrial processing, still need to be improved for conventional batch process. Herein, towards fast and cost-effective integration, Gao and coworker successfully demonstrated a hydrothermal based continuous flow synthesis (CFS) which enables a stable and consecutive mass transport generated within the substrate channels (Figure 5 (c)).[63] The special heating and cooling circulation effectively suppresses the growth of homogeneously formed nuclei by confining the crystal growth

within honeycomb substrate, giving rise to an enhanced average growth rate and improved precursor utilization efficiency that can be hardly achieved from conventional batch process.[64] The pumping flow rate was found to be a crucial parameter that not only determines the nano-array's distribution uniformity but also sustains a stable and fast growth rate. It is thus reasonable to expect the with the microwave heating combined, this green, low-cost, and fast hydrothermal synthesis can potentially become a promising scalable integration strategy that can be extended to the fabrication of a variety of TMO nano-array andopens up the possibility of realizing the practical scalable nanomanufacturing of 3-D nano-array integrated monolithic devices.

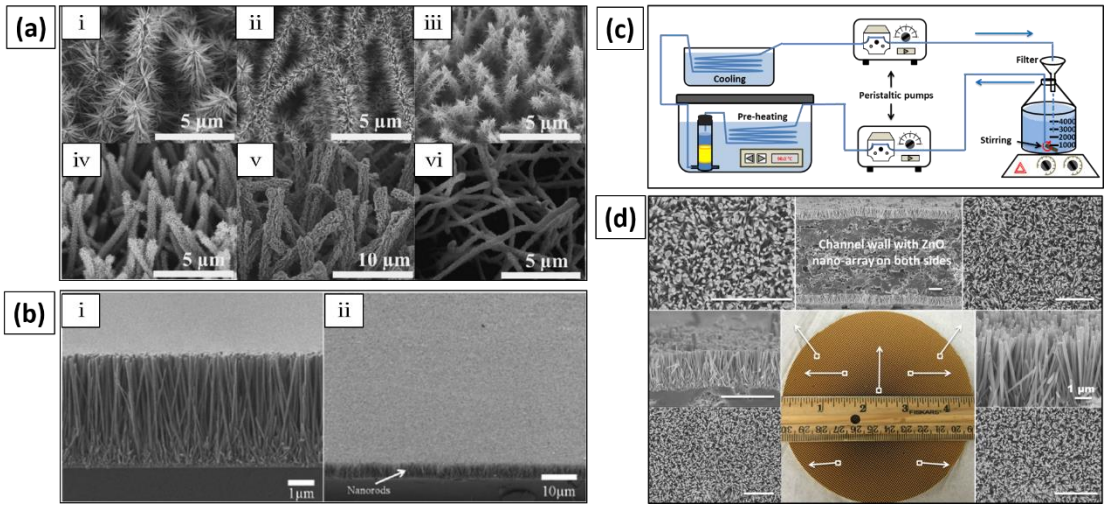

Figure 5 (a) (ⅰ) and (ⅱ) 3-D branched CuO/Co_3O_4 core-shell nanowire array and $NiSi_x/NiCo_2O_4$ core-shell nanowire array grown on Ni foam; (ⅲ) 3-D branched $CuO/Cu_xCo_{3-x}O_4$ core-shell nanorod array on Cu foam; (ⅳ) (ⅴ) and (ⅵ) 3-D branched CuO/Co_3O_4 core-shell nanorod array, CuO/NiO core-shell nanorod array and $NiSi_x$/NiO core-shell nanowire arrays on Cu foam. Reproduced with permission from reference 46. (b) (ⅰ) cross-sectional view and (ⅱ) low-magnification SEM images of fast integrated and impurities free ZnO nanorods array on ITO substrate. Reproduced with permission from reference 48. (c) Experimental setup of continuous flow synthesis for scalable integration of ZnO nanorod array on 3-D honeycomb cordierite. (d) Uniformly distributed ZnO nanorod array on monolithic substrate fabricated by continuous flow synthesis.

Functional Monolithic Nano-array Devices

Heterogeneous catalysis plays an essential role in clean energy utilization, conversion and storage, and environmental protection and remediation. Nowadays, the implementation of fuel economy standard and development of low temperature combustion technology call for new generation exhaust after-treatment system for mobile and stationary emissions to achieve 90% emission conversion at temperatures of 150^o C or lower. As the core part of catalytic converter, the state-of-the-art wash-coating based monolithic catalysts are used in current automotive industry, lacking well-defined structure configurations, highly dependent on the large amount usage of Pt-group metal (PGM). Gao and coworkers demonstrated and proved that replacing

the wash-coated power-form catalysts with integrated nano-array catalysts on commercialized honeycomb substrate is able to significantly improves the surface area and spatial usage, reduce the agglomeration of catalytic active phase and enhance the materials utilization efficiency (Figure 6 (a)).[43,65] With comparable catalytic performance, the metal oxide and platinum usage for nano-array catalyst was claimed to be 10~40 times less than powder-form wash-coated catalyst. From the catalytic gas reaction viewpoint, densely-packed nano-array catalysts with ordered macropores between individual nanostructures provide a shorter diffusion pathway and thus improved gas-solid phase interaction. In addition to the exceptional material usage, rational manipulation of nano-array structure such as adjusting dimensionality and shape leads to a tunable catalytic performance towards toxic gas removal. When hierarchically decorated with functional components or properly doping with other transition metals into the structure lattice, nano-array catalysts are able to exhibit enhanced catalytic performance. For instance, Ren reported that a series of spinel $M_xCo_{3-x}O_4$ (M = Co, Ni, Zn) nano-array catalysts have been monolithically integrated on 3-D honeycomb substrate via the low temperature hydrothermal approach (Figure 6 (b)).[66,67] These monolithic nano-array catalysts demonstrated significantly enhanced catalytic performance towards hydrocarbon combustion. Interestingly, doping of Ni into Co_3O_4 nano-array was discovered to promote the activity of lattice oxygen and the formation of catalytically favorable but less thermally stable carbonate species on the surface which are responsible for the enhanced reaction kinetics. Though this enhancement of catalytic activity needs to be balanced with sacrificed thermal stability brought by Ni incorporation, monolithic Co_3O_4 based nano-array catalyst still emerges as a guidance of rational catalyst design for low temperature emission control technology.

Besides the promotion effect given rise by dopant incorporation, design of hierarchically architectured nano-array catalysts also lead to a remarkable improvement of catalytic performance. Duan and coworkers investigated the hierarchically integration of $Co_{3-x}Fe_xO4$ nano-array on metal substrate which can be directly used as monolithic structured catalysts for chemical refinement (Figure 6 (c)).[68] Notably, Fe doping allows the appearance of abundant new reactive sites, and hierarchical design of nano-array structure enables exposure of more reactive planes. Furthermore, the LDH nanosheet array directly grown on the surface of substrate not only contributes to the catalytic activity, but also performs as anchor for nanowire array demonstrating a superior catalytic performance for selective oxidation of styrene with good recyclability.

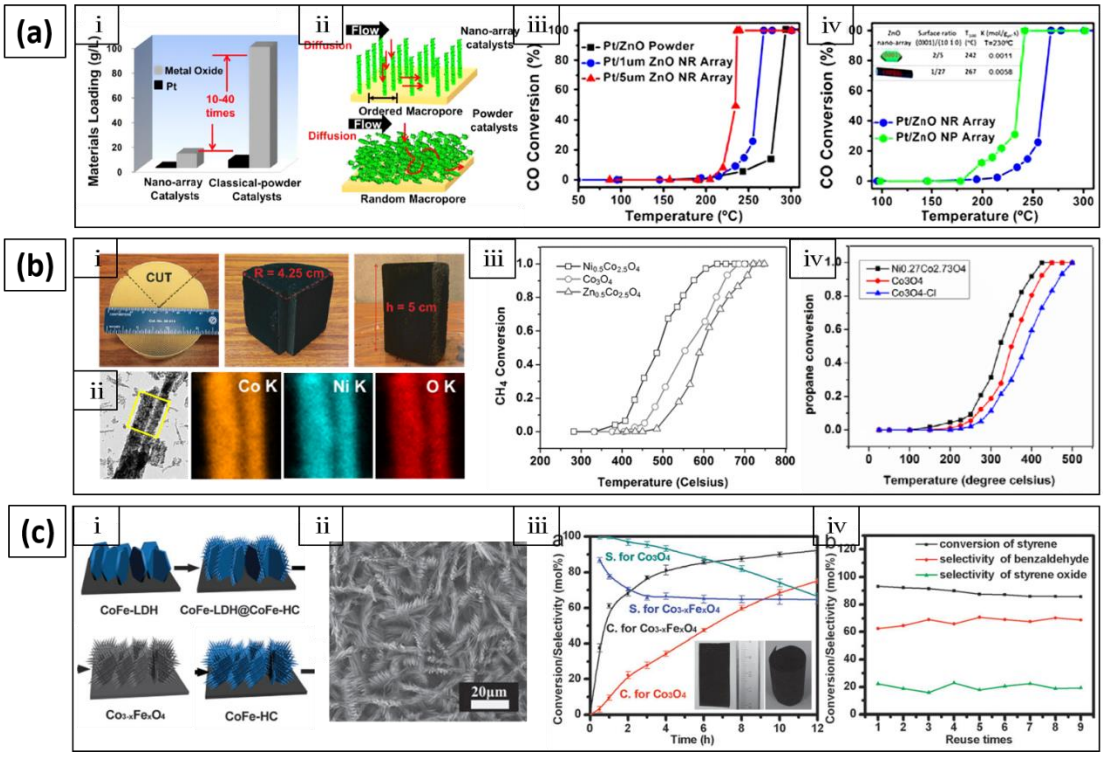

Figure 6 (a) (ⅰ) Ultrahigh materials utilization efficiency of monolithic nano-array catalysts compared to classical powder-form catalysts; (ⅱ) schematic illustration of gas-solid phase interactions in nano-array configuration and powder-form catalysts; (ⅲ) catalytic CO oxidation performance of powder-form Pt/ZnO catalyst, 1 μm long and 5 μm long Pt/ZnO nano-array catalysts; (ⅳ) catalytic CO oxidation performance of Pt/ZnO nanorod array and Pt/ZnO nanoplate array. Reproduced with permission from reference 43. (b) (ⅰ) Photograph of commercialized monolithic cordierite before and after Co_3O_4 nanowire array deposition. Reproduced with permission from reference 66; (ⅱ) TEM image and STEM mapping of Ni doped $Ni_{0.27}Co_{2.73}O_4$ nanowire. Reproduced with permission from reference 67; (ⅲ) tunable catalytic methane oxidation performance of Co_3O_4 nano-array catalysts enabled by Ni and Zn incorporation. Reproduced with permission from reference 66; (ⅳ) catalytic propane oxidation performance of various Co_3O_4 based nano-array catalysts. Reproduced with permission from reference 67. (c) (ⅰ) and (ⅱ) Schematic illustration of multistep growth process and SEM image of hierarchical $Co_{3-x}Fe_xO_4$ nano-array on iron substrate; (ⅲ) styrene conversion and benzaldehyde selectivity as function of time for nano-array catalyst, inset: optical images of $Co_{3-x}Fe_xO_4$ nano-array on iron substrate as structured catalyst; (ⅳ) the recyclability of the $Co_{3-x}Fe_xO_4$ nano-array structured catalysts. Reproduced with permission from reference 67.

Development of high performance gas sensors represents the technological importance for air quality monitoring and control in public health and safety, automotive and stationary energy industries. Good sensitivity, selectivity and fast response are among the required features of a highly efficient gas sensor device enabling a precise and in-time detection of target gaseous component(s) in a complicated environment. However, the morphology and microstructure of sensing materials have critical impact on the performance of gas sensor. For example, gas

sensors based on dense film lack the desired sensitivity and stability under harsh conditions because the grain boundary can be easily altered with variant temperature. In contrast, thermodynamically stable 1-D nanostructures directly grown on the surface of substrate, possessing a high surface-to-volume ratio, is kinetically favorable to the surface reaction [69,70] A maximum response even can be expected when the lateral dimensions of 1-D nanostructures become comparable to the Debye length [71]. Assembly of 1-D nanostructures into 3-D arrangement with well-defined structure is able to prevent the active sites agglomeration and the controlled porosity between individual nanostructures facilitates the gas molecules adsorption. Therefore, engineering delicate 1-D nano-array to show large surface area and porosity is emerging as a promising design strategy for fabricating high performance gas sensor devices.

Despite various options of sensing materials, transition metal oxides are still the most popular materials being studied due to their diversity of valance states. Zhang and coworkers demonstrated a facile method to prepare CeO_2 nanotube array with well controlled geometry on Si wafer by using ZnO nanorod template and H_2-TPR removal process (Figure 7 (a)).[72] This porous CeO_2 nanotube array integrated monolithic sensor device can be directly employed for oxygen detection, exhibiting great sensitivity, rapid response capability and excellent robustness. Recently, high temperature toxic gas sensor has drawn great attention due to the demanded applications in harsh operation conditions. Although noble metals are being extensively used to purposely enhance the sensitivity of gas sensor, it is of great importance to develop non-noble-metal based substitution from the perspective of material and environmental sustainability. Lin and coworkers investigated the high temperature carbon monoxide sensing performance of perovskite/Ga_2O_3 nano-array integrated gas sensor (Figure 7 (b)).[73] Hydrothermally prepared β-Ga_2O_3 nanorod array was decorated with uniformly distributed $La_{0.8}Sr_{0.2}FeO_3$ (LSFO) nanoparticles with diameter of a few nanometers. The catalytic spill-over effect and formation of p-n junction were discovered in LSFO decorated Ga_2O_3 nanorod array, giving rise to the significantly enhanced CO sensitivity than pristine Ga_2O_3 nanorod array while poor sensitivity was observed on LSFO film itself. Moreover, LSFO/Ga_2O_3 nano-array sensor, showing comparable sensitivity to Pt-Ga_2O_3 nano-array sensor, displays shortened response time at the same CO concentration. The demonstrated non-noble-metal LSFO/Ga_2O_3 nano-array may lead to the realization of stable and high efficient nano-array sensor devices for high-temperature gas detection. 1-D ZnO nanostructures have been widely employed for fabricating high performance sensor devices due to their unique physical properties. Gao and coworkers reported ZnO/(La, Sr)CoO_3 core-shell nano-array based humidity sensor, the photo-illumination induced current of which is strongly associated with the amount of physically adsorbed water molecules (Figure 7 (c)).[74] In a similar design strategy, ZnO /(La, Sr)MnO_3 (LSMO) core-shell nano-array was also investigated as high efficient magnetic device (Figure 7 (d)).[75] The 3-D LSMO thin film exhibits a thickness-dependent ferromagnetic-superparamagnetic transition owing to the surface dispersion effect. In light of these demonstrated intriguing properties, nano-array architectures have opened up a new avenue of engineering high-performance sensor devices for a variety of applications.

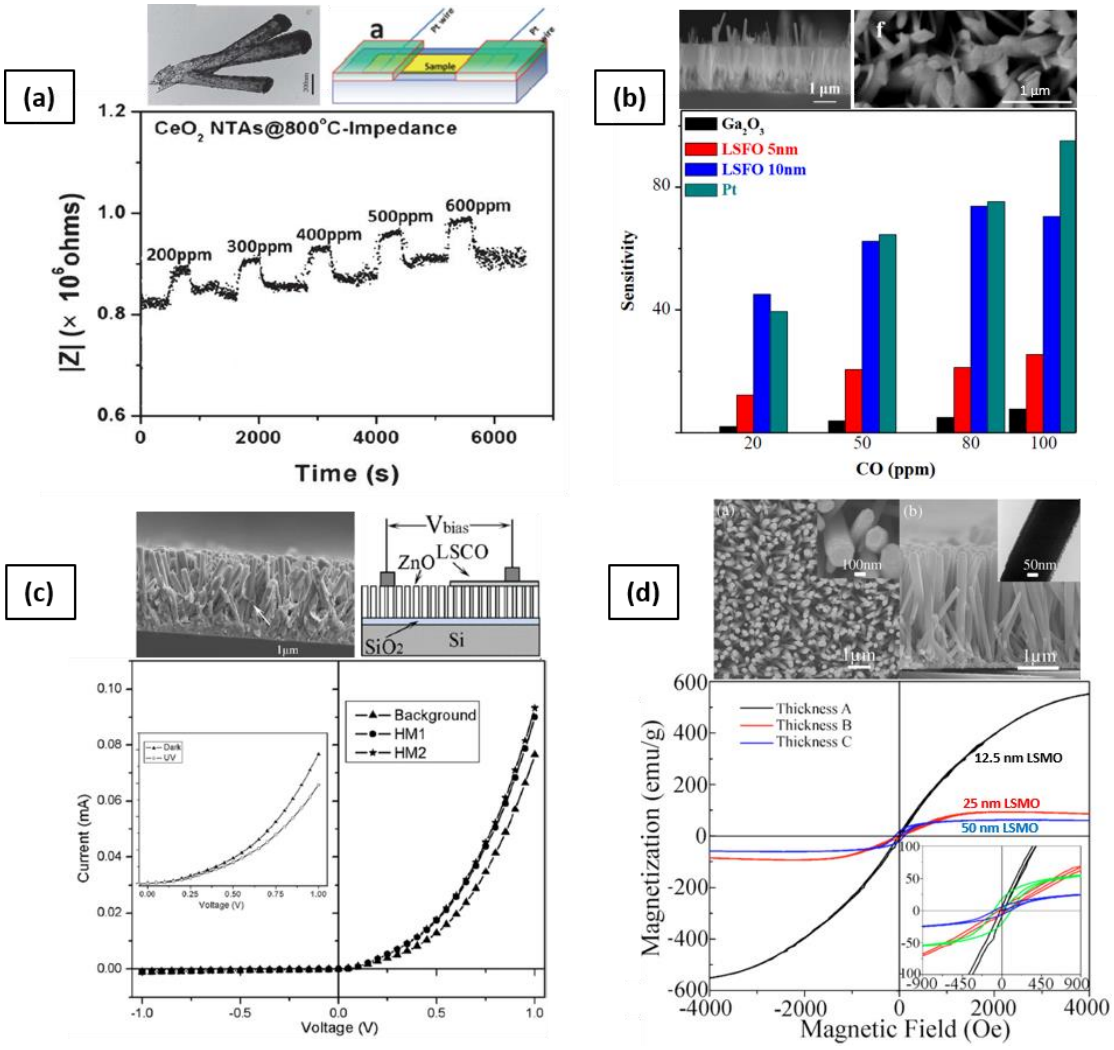

Figure 7 (a) O_2 response plot of CeO_2 nanotube arrays on Si substrate, inset: (left) TEM image of CeO_2 nanotube, (right) Schematic illustration of CeO_2 nanotube array based O_2 sensor device. Reproduced with permission from reference 72. (b) Sensitivity versus CO concentrations of various type of nanorod arrays based gas sensors tested at 500 ˚C, inset: (left) cross-sectional view SEM image of GaOOH nanorod array before calcination, (right) top view SEM image of β-Ga_2O_3 nanorod after calcination at 1000 ˚C. Reproduced with permission from reference 73. (c) Current-voltage (*I*-*V*) measurement of LSCO/ZnO nano-array upon UV irridation in different humidities, inset: (left) SEM image of ZnO/LSCO core-shell nanorod array, (right) schematic illustration of *I*-*V* measurement setup. Reproduced with permission from reference 74. (d) Typical M-H hysteresis curves of LSMO film with different thickness on ZnO nanorod array measured at 80 K with magnetic field applied parallel to the film. Inset: (bottom corner) detailed M-H hysteresis curves at low magnetic field, (top left) top-view and (top right) cross-sectional view of LSCO/ZnO nanofilm/nanorod arrays. Reproduced with permission from reference 75.

Much effort has also been devoted to developing high efficient energy conversion and storage devices which represent an important renewable energy source in the future. As a new class of monolithic devices, metal oxide nano-array integrated electrodes have drawn extensive

interests due to the exceptional performance originated from the novel 1D nanostructures. In the electrochemical systems such as batteries made from monolithic nano-arrays, the high specific capacity and good cycle performance are most intriguing properties that could potentially revolutionize the energy storage technology. 1-D nano-arrays not only provide large electrochemically active surface area, but also are considered as natural superhighway to facilitate charge carrier transport.

Metal oxide nano-array integrated on conductive substrates has been demonstrated as a unique and efficient electrode configuration with direct contact between individual active nanostructure and charge collector to favor electrochemical reactions. 3-D integration of TMO nano-array on flexible substrates, such as macroporous carbon cloth [76,77,78,79,80] and metal foam,[81,82,83,84,85,86,87] further reveals the potential of using monolithic nanoarray configuration to achieve high capacity, decent rate performance and excellent cycling stability. The monolithic nano-array configuration will very likely become the key to fabricating high performance devices for flexible and portable electronics. As an example, Gao and coworkers investigated the performance of WO_3 nanowire array/carbon cloth integrated electrode for energy storage devices (Figure 8 (a)).[88] Uniform and densely packed WO_3 nanowire array was hydrothermally grown on flexible carbon fibers. Such binder free electrode shows extraordinary electrochemical and cycling performance without deterioration at the increasing bending angle. The integrated electrode was further designed by depositing a layer of SnO_2 onto WO_3 nanowire array.[89] The amorphous SnO_2 nano-shell functions as charge transport medium at electrolyte/electrode interface and yields an enhanced functional performance observed in WO_3@SnO_2 core-shell integrated electrode.

As a typical example of delicate muti-component nano-array device, Xing and coworkers reported a ternary composite photoelectrodes composed of ordered TiO_2 nanotube arrays (TNTs), transparent reduced graphene oxide (RGO) film, and randomly distributed CdS nanocrystallites (Figure 8 (b)).[90] In this hierarchical material system of multiple components, each individual nanostructure component plays a designated role in photon sensing and capturing, charge separation and collection, which leads to a significantly enhanced visible-light-driven photoelectrochemical activity. Monolithic nano-array devices should not be confined by the geometric structure of substrate. Integration of nano-array onto nanoscale surface opens up the realization of novel functional monolithic device assembled by plenty of mini ones. We recently developed a novel photocatalyst composed of photocatalytically active ZnO nanowire array rooted on the surface of magnetic γ -Fe_2O_3@SiO_2 spheres with diameter of hundreds nanometer (Figure 8 (c)).[91] The ease of dispersion and recyclability has made it a good candidate as next generation high-efficiency photocatalyst for water treatment. This hierarchically structured photocatalyst obtained through manipulation of functional nanostructures within nanoscale represents a promising integration strategy of functional nanodevice with a merit can be extended to the design of other energy and environmental relevant nano-array devices.

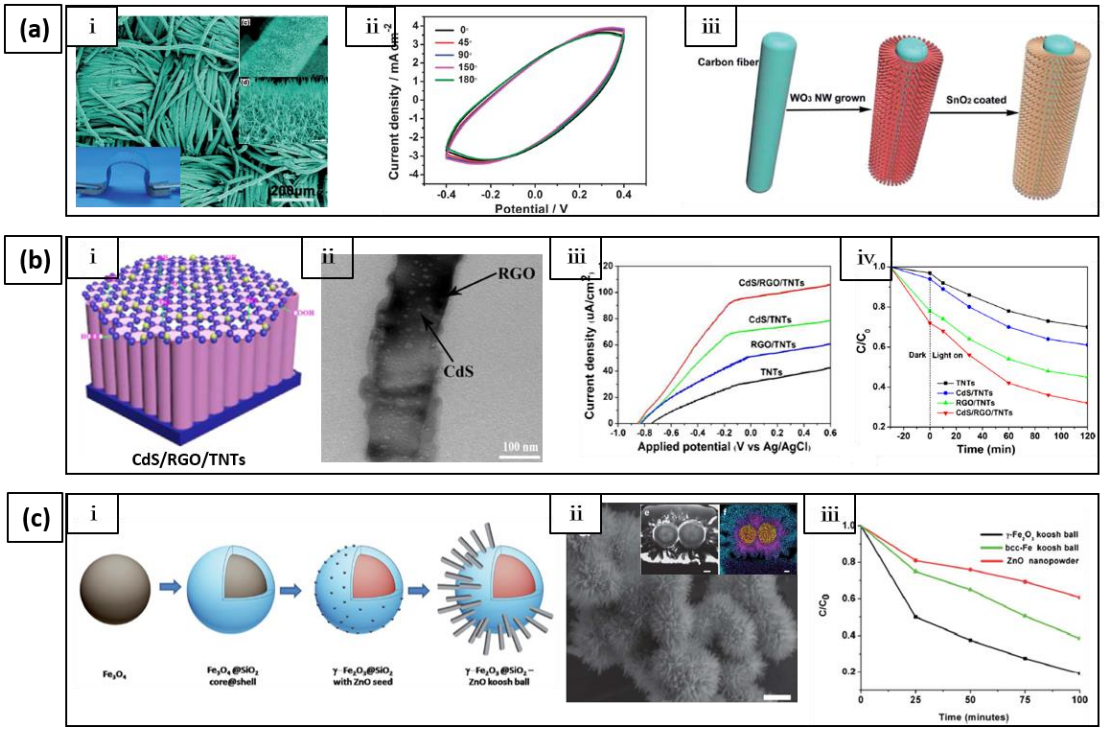

Figure 8 (a) (ⅰ) SEM image of WO_3 nanowire arrays integrated carbon cloth. Inset: (Left) photograph of flexible WO_3 nanowire array based supercapacitor device, (right) SEM image of WO_3 nano-array on carbon cloth at different magnifications; (ⅱ) CV curves of WO_3 nano-array supercapacitor collected at the scan rate of 100 mV s^{-1} at different bending angles; (ⅲ) schematic illustration of the synthesis of WO_3@SnO_2 hierarchical nanowire arrays on carbon cloth. Reproduced with permission from reference 88 and 89. (b) (ⅰ) Schematic diagram of the ternary CdS/RGO/TNTs hybrids nano-array based photoelectrode; (ⅱ) TEM image of individual CdS/RGO/TNT; (ⅲ) linear-sweep voltammograms at scanning rate of 5 mV/s; (ⅳ) visible-light-driven photocatalytic degradation of MB as function of time over CdS/RGO/TNTs and corresponding single or binary components. Reproduced with permission from reference 90. (c) (ⅰ) The schematic illustration of the growth process of γ-Fe_2O_3@SiO_2-ZnO three-layered koosh ball nanoarchitecture; (ⅱ) SEM image of typical koosh ball architectures. Inset: STEM image of FIB milled koosh ball nanoarchitecture and corresponding EDX element mapping; (ⅲ) photocatalytic degradation of Rhodamine B by ZnO nanopowders, bcc-Fe@SiO_2-ZnO koosh balls andγ-Fe_2O_3@SiO_2-ZnO koosh balls. Reproduced with permission from reference 91.

Conclusions and perspectives

This highlight presents the latest work and typical examples of nano-array integrated devices for energy and environmental applications in perspectives of materials design principles and strategies of scalable self-assembly. The unique properties of nanostructures, especially 1-D nanoscale building blocks, have triggered tremendous amount of studies in the applications of catalysis, sensing, and photoelectrochemical reactions. 3-D integration of nano-array on structurally diverse substrates demonstrates a variety of benefits that may lead to the revolutionary development of high-efficiency and cost-effective functional nano-array devices.

The advantages of nano-array integrated monolithic device configurations are listed as follows.

- The well-defined nano-array configuration provides optimized surface area and uniformly distributed active sites on the 3-D substrates;
- High materials utilization efficiency of well-spaced and immobilized nanostructures avoids compromised performance that may be caused by material agglomeration;
- The well-defined nano-array configuration allows for tunable performance by selecting material composition, size, shape and structure, and designing the form of nano-ensembles (or nanoarchitectures) and enables the optimum correlation between their geometrical, structural and functional properties.

In perspective of catalysis and sensing, 3-D nano-array integrated honeycomb cordierites have displayed enhanced gas-solid or liquid-solid interactions and good catalytic activities for gas and liquid phase reactions, holding a great promise as new generations of monolithic catalysts, sensors and relevant devices for exhaust removal, environmental remediation and sensing, and chemical refining. The tuning of catalytic activity through manipulation of constituted nanostructure geometry, size and composition also provides an important route for design of new class nano-array based catalytic devices for energy conversion and sensor applications. However, one major concern over the applicability and commercial viability of metal oxide nano-array configured catalytic and functional device platforms is the normally compromised thermal and hydrothermal stability. For example, Co_3O_4 nano-array catalyst suffers severe structure deterioration during hydrothermal aging, and excessive Ni incorporation leads to poor stability of Co_3O_4 at temperature above 600 °C.[66,67] It is thus important to design and search more stable array configured system with proper material structure and composition design. With the growing demand and rapid development of energy efficient technologies for energy conversion and utilization such as low-temperature-combustion engines [92] and photo-thermal renewable energy generation reactors,[93] low-temperature catalysis is becoming more and more attractive for both gas phase and liquid phase reactions. It is necessary to further improve the catalytic activity of nano-array catalysts, especially low-temperature activity, by extracting the scientific understanding of the gas-solid interaction that dominates the reaction kinetics. Moreover, since the inevitable use of noble metal to achieve expected low-temperature activity, the interaction between noble metal and metal oxide nano-array should be systematically investigated to reduce materials usage and optimize the performance of nano-array catalysts.
For electrochemical energy storage and conversion systems, relatively poor conductivity of metal oxides is still the major hurdle of pursuing electrodes with long lifecycle despite of the high energy capacity, fast charge-discharge rate performance and good capability of strain release enabled by the above mentioned merits of nano-array configuration.[94,95] While conductive electron collectors are becoming dominant substrates nowadays, rational incorporation of carbon based nanoscale subunits into 3-D metal oxide nano-arrays to better construct electron transport pathways should still be considered if longer lifecycle is desired.

For heterogeneous catalysis, the hydrothermally grown metal oxide nanostructure arrays are intrinsically active, which offers an opportunity to avoid complex industrial wash-coating

process and gives rise to more concise manufacture techniques.[96] In perspective of environmental protection, the green synthetic approach and the robustness of nano-array structure prevent harmful materials from diffusing into eco-system. Therefore, to pursue the demonstrated catalytic performance and other benefits mentioned previously enabled by nano-array configuration, a tradeoff should be made between developing efficient scale-up production strategy and lowering the overall cost of nano-array devices. As one of the promising scalable integration strategies for nano-array devices, the production quality and efficiency of low temperature solvothermal synthesis are usually hindered by poor growth rate, low precursor usage, and non-uniform coverage of nano-array structures in confined spaces of 3-D substrates. Through optimizing growth parameters and proper introduction of mechanical agitation, this hurdle can be mitigated. However, it is necessary and still a challenging task to develop scientific understanding of mass transport in aqueous solution environment and new reactor design to meet the synthetic and production requirements of structurally sophisticated substrates.

Despite all these potential applications of nano-array devices, there is still a long way for the current laboratory synthetic approaches to be truly generic in industry. The manufacturing efficiency needs to be greatly enhanced and the deposition of materials needs more precise control on the large scale. The cost-effective hydrothermal growth accompanied by alternative/external heating/energy sources other than bulk resistive heating will very likely to accelerate the manufacturing, such as microwave heating, laser heating, external energy assistance through ultrasound and electrical field. For complex hierarchical nanostructures assembly on the industrially relevant scale, however, the cost and the sophistication of fabrication process needs to be further reduced. Furthermore, a collection of commercially-viable and new manufacturing standards and protocols are needed to be established with respect to various specific market applications of the nano-array integrated materials and devices. Concurrently, these establishments must be supported with robust and quantitative system-level economic/cost analysis and modeling.

In summary, we hope the design concept and integration principles illustrated in this highlight could provide some important guidance of rational materials design for exploration of high performance monolithic nano-array devices for advanced energy and environmental technologies that could impact a broad spectrum of business sectors including automotive, chemical, energy, mechanical, petrochemical, and biotechnology industries.

Acknowledgement: The authors are grateful for the financial support from the US Department of Energy (Award Nos. DE-EE0006854 and DE-FE0011577) and the US National Science Foundation (Award No. CBET-1344792). S. W. would like to acknowledge the partial support from a FEI Graduate Fellowship.

1 Z. Zhang, X. Sun, M. Dresselhaus, J. Y. Ying and J. Heremans, *Physical Review B*, 2000, 61, 4850.

2 L. Vayssieres, C. Sathe, S. M. Butorin, D. K. Shuh, J. Nordgren and J. Guo, Advanced Materials, 2005, 17, 2320-2323.
3 Y. Gu, I. L. Kuskovsky, M. Yin, S. O'Brien and G. Neumark, mh, 2004, 2, 2r2.
4 N. Singhania, E. Anumol, N. Ravishankar and G. Madras, Dalton Transactions, 2013, 42, 15343-15354.
5 R. Gao, D. Zhang, P. Maitarad, L. Shi, T. Rungrotmongkol, H. Li, J. Zhang and W. Cao, The Journal of Physical Chemistry C, 2013, 117, 10502-10511.
6 X. Mou, B. Zhang, Y. Li, L. Yao, X. Wei, D. S. Su and W. Shen, Angewandte Chemie International Edition,
2012, 51, 2989-2993.
7 Q.-X. Gao, X.-F. Wang, J.-L. Di, X.-C. Wu and Y.-R. Tao, Catalysis Science & Technology, 2011, 1, 574-577.
8 K. Zhou, X. Wang, X. Sun, Q. Peng and Y. Li, Journal of Catalysis, 2005, 229, 206-212.
9 P.-X. Gao, P. Shimpi, H. Gao, C. Liu, Y. Guo, W. Cai, K.-T. Liao, G. Wrobel, Z. Zhang and Z. Ren, International journal of molecular sciences, 2012, 13, 7393-7423.
10 J. Jiang, Y. Li, J. Liu and X. Huang, Nanoscale, 2011, 3, 45-58.
11 R. S. Devan, R. A. Patil, J. H. Lin and Y. R. Ma, Advanced Functional Materials, 2012, 22, 3326-3370.
12 P. Poudel and Q. Qiao, Nanoscale, 2012, 4, 2826-2838.
13 L. Mai, X. Tian, X. Xu, L. Chang and L. Xu, Chemical reviews, 2014, 114, 11828-11862.
14 Y. Wang, J. Zeng, J. Li, X. Cui, A. M. Al-Enizi, L. Zhang and G. Zheng, Journal of Materials Chemistry A, 2015, 3, 16382-16392.
15 X. Liu, M.-H. Liu, Y.-C. Luo, C.-Y. Mou, S. D. Lin, H. Cheng, J.-M. Chen, J.-F. Lee and T.-S. Lin, Journal of the American Chemical Society, 2012, 134, 10251-10258.
16 H. Li, X. Wang, J. Xu, Q. Zhang, Y. Bando, D. Golberg, Y. Ma and T. Zhai, Advanced Materials, 2013, 25, 3017-3037.
17 X. Sheng, D. He, J. Yang, K. Zhu and X. Feng, Nano letters, 2014, 14, 1848-1852.
18 C. J. Lin, S.-J. Liao, L.-C. Kao and S. Y. H. Liou, Journal of hazardous materials, 2015, 291, 9-17.
19 S. Wang, Y. Yu, Y. Zuo, C. Li, J. Yang and C. Lu, Nanoscale, 2012, 4, 5895-5901.
20 Z. Ren, Y. Guo and P.-X. Gao, Catalysis Today, 2015, 258, 441-453.
21 B. Weng, S. Liu, Z.-R. Tang and Y.-J. Xu, Rsc Advances, 2014, 4, 12685-12700.
22 M. Wang, D. Zheng, M. Ye, C. Zhang, B. Xu, C. Lin, L. Sun and Z. Lin, small, 2015, 11, 1436-1442.
23 S.-Y. Chen, W. Song, H.-J. Lin, S. Wang, S. Biswas, M. Mollahosseini, C.-H. Kuo, P.-X. Gao and S. L. Suib, ACS Applied Materials & Interfaces, 2016. DOI: 10.1021/acsami.6b00578
24 S. Liu, Z.-R. Tang, Y. Sun, J. C. Colmenares and Y.-J. Xu, Chemical Society Reviews, 2015, 44, 5053-5075.
25 F. X. Xiao, J. Miao, H. B. Tao, S. F. Hung, H. Y. Wang, H. B. Yang, J. Chen, R. Chen and B. Liu, Small, 2015, 11, 2115-2131.
26 Y. Lim, J. Son and J.-S. Rhee, Ceramics International, 2013, 39, 887-890.
27 J. Trasobares, F. Vaurette, M. François, H. Romijn, J.-L. Codron, D. Vuillaume, D. Théron and N. Clément, Beilstein journal of nanotechnology, 2014, 5, 1918-1925.
28 A. R. Madaria, M. Yao, C. Chi, N. Huang, C. Lin, R. Li, M. L. Povinelli, P. D. Dapkus and C.

Zhou, Nano letters, 2012, 12, 2839-2845.
29 L. Li, Y. Zhang, X. Liu, S. Shi, X. Zhao, H. Zhang, X. Ge, G. Cai, C. Gu and X. Wang, Electrochimica Acta, 2014, 116, 467-474.
30 L. Yu, L. Zhang, H. B. Wu, G. Zhang and X. W. D. Lou, Energy & Environmental Science, 2013, 6, 2664-2671.
31 G. Cai, J. Tu, D. Zhou, X. Wang and C. Gu, Solar Energy Materials and Solar Cells, 2014, 124, 103-110.
32 R. Chen, H.-Y. Wang, J. Miao, H. Yang and B. Liu, Nano Energy, 2015, 11, 333-340.
33 Y. Hou, F. Zuo, A. P. Dagg, J. Liu and P. Feng, Advanced Materials, 2014, 26, 5043-5049.
34 F. Zheng, H. Lu, M. Guo, M. Zhang and Q. Zhen, Journal of Materials Chemistry C, 2015, 3, 7612-7620.
35 Y. Wang, Y.-Z. Zheng, S. Lu, X. Tao, Y. Che and J.-F. Chen, ACS applied materials & interfaces, 2015, 7, 6093-6101.
36 W.-Q. Wu, B.-X. Lei, H.-S. Rao, Y.-F. Xu, Y.-F. Wang, C.-Y. Su and D.-B. Kuang, Scientific reports, 2013, 3.
37 W.-Q. Wu, Y.-F. Xu, C.-Y. Su and D.-B. Kuang, Energy & Environmental Science, 2014, 7, 644-649.
38 Z. Gu, R. Wang, H. Nan, B. Geng and X. Zhang, Journal of Materials Chemistry A, 2015, 3, 14578-14584.
39 D. Guo, Y. Luo, X. Yu, Q. Li and T. Wang, Nano Energy, 2014, 8, 174-182.
40 D. Jian, P.-X. Gao, W. Cai, B. S. Allimi, S. P. Alpay, Y. Ding, Z. L. Wang and C. Brooks, Journal of Materials Chemistry, 2009, 19, 970-975.
41 M. Shao, F. Ning, M. Wei, D. G. Evans and X. Duan, Advanced Functional Materials, 2014, 24, 580-586.
42 J. Shi, C. Sun, M. B. Starr and X. Wang, Nano letters, 2011, 11, 624-631.
43 Y. Guo, Z. Ren, W. Xiao, C. Liu, H. Sharma, H. Gao, A. Mhadeshwar and P.-X. Gao, Nano Energy, 2013, 2, 873-881.
44 Y. Guo, Z. Zhang, Z. Ren, H. Gao, and P.-X. Gao. Catalysis Today, 2012, 184, 178-183.
45 S. Wang, Z. Ren, W. Song, Y. Guo, M. Zhang, S. L. Suib and P.-X. Gao, Catalysis Today, 2015, 258, 549-555.
46 Q. Zhang, J. Wang, J. Dong, F. Ding, X. Li, B. Zhang, S. Yang and K. Zhang, Nano Energy, 2015, 13, 77-91.
47 L. Schlur, A. Carton, P. Lévêque, D. Guillon and G. v. Pourroy, The Journal of Physical Chemistry C, 2013, 117, 2993-3001.
48 L. Schlur, A. Carton and G. Pourroy, Chemical Communications, 2015, 51, 3367-3370.
49 Y. Lei, J. Li, Y. Wang, L. Gu, Y. Chang, H. Yuan and D. Xiao, ACS applied materials & interfaces, 2014, 6, 1773-1780.
50 P. K. Panigrahi and A. Pathak, Science and Technology of Advanced Materials, 2016.
51 B. N. Rao, P. Muralidharan, P. R. Kumar, M. Venkateswarlu and N. Satyanarayana, Int. J. Electrochem. Sci, 2014, 9, 1207-1220.
52 L. Shi, C. Yang, X. Su, J. Wang, F. Xiao, J. Fan, C. Feng and H. Sun, Ceramics International, 2014, 40, 5103-5106.
53 J. Pan, M. Li, Y. Luo, H. Wu, L. Zhong, Q. Wang and G. Li, Materials Research Bulletin, 2016, 74, 90-95.

54 A. Pimentel, D. Nunes, P. Duarte, J. Rodrigues, F. Costa, T. Monteiro, R. Martins and E. Fortunato, The Journal of Physical Chemistry C, 2014, 118, 14629-14639.
55 I. Bilecka and M. Niederberger, Nanoscale, 2010, 2, 1358-1374.
56 Y.-J. Zhu and F. Chen, Chemical Reviews, 2014, 114, 6462-6555.
57 J. Tang, J. Chai, J. Huang, L. Deng, X. S. Nguyen, L. Sun, T. Venkatesan, Z. Shen, C. B. Tay and S. J. Chua, ACS applied materials & interfaces, 2015, 7, 4737-4743.
58 Q. Li, W. Cao, J. Lei, X. Zhao, T. Hou, B. Fan, D. Chen, L. Zhang, H. Wang and H. Xu, Crystal Research and Technology, 2014, 49, 298-302.
59 X. Ge, K. Hong, J. Zhang, L. Liu and M. Xu, Materials Letters, 2015, 139, 119-121.
60 L. Liu, K. Hong, X. Ge, D. Liu and M. Xu, The Journal of Physical Chemistry C, 2014, 118, 15551-15555.
61 L.-Y. Chen and Y.-T. Yin, Crystal Growth & Design, 2012, 12, 1055-1059.
62 J. Yeo, S. Hong, M. Wanit, H. W. Kang, D. Lee, C. P. Grigoropoulos, H. J. Sung and S. H. Ko, Advanced Functional Materials, 2013, 23, 3316-3323.
63 S. Wang, Y. Wu, Y. Guo, M. Zhang, A. Kinstler, Z.Y. Ren, T.F. Lu and P.-X. Gao, Scalable Continuous Flow Synthesis of ZnO Nanorod Arrays in 3D Ceramic Honeycomb Substrate, 2016, to be submitted.
64 W. Xiao, Y. Guo, Z. Ren, G. Wrobel, Z. Ren, T. Lu and P.-X. Gao, Crystal Growth & Design, 2013, 13, 3657-3664.
65 Z. Ren, Y. Guo, Z. Zhang, C. Liu and P.-X. Gao, Journal of Materials Chemistry A, 2013, 1, 9897-9906.
66 Z. Ren, V. Botu, S. Wang, Y. Meng, W. Song, Y. Guo, R. Ramprasad, S. L. Suib and P. X. Gao, Angewandte Chemie International Edition, 2014, 53, 7223-7227.
67 Z. Ren, Z. Wu, W. Song, W. Xiao, Y. Guo, J. Ding, S. L. Suib and P.-X. Gao, Applied Catalysis B: Environmental, 2016, 180, 150-160.
68 J. Sun, Y. Li, X. Liu, Q. Yang, J. Liu, X. Sun, D. G. Evans and X. Duan, Chemical Communications, 2012, 48, 3379-3381.
69 X. Chen, C. K. Wong, C. A. Yuan and G. Zhang, Sensors and Actuators B: Chemical, 2013, 177, 178-195.
70 Z. Ren, Y. Guo, C.-H. Liu and P.-X. Gao, Frontiers in chemistry, 2013, 1.
71 C. Wang, L. Yin, L. Zhang, D. Xiang and R. Gao, Sensors, 2010, 10, 2088-2106.
72 Z. Zhang, H. Gao, W. Cai, C. Liu, Y. Guo and P.-X. Gao, Journal of Materials Chemistry, 2012, 22, 23098-23105.
73 H.-J. Lin, J.P. Baltrus, H. Gao, Y. Ding, C.-Y. Nam, P. Ohodnicki and P.-X. Gao, Perovskite Nanoparticle Sensitized Ga_2O_3 Nanorod Arrays for CO Detection at High Temperature, ACS Applied Materials & Interfaces, 2016, in revision.
74 H. Gao, W. Cai, P. Shimpi, H.-J. Lin and P.-X. Gao, Journal of Physics D: Applied Physics, 2010, 43, 272002.
75 H. Gao, M. Staruch, M. Jain, P.-X. Gao, P. Shimpi, Y. Guo, W. Cai and H.-j. Lin, Applied Physics Letters, 2011, 98, 123105.
76 Q. Ke, C. Guan, M. Zheng, Y. Hu, K.-h. Ho and J. Wang, Journal of Materials Chemistry A, 2015, 3, 9538-9542.
77 C. Wu, J. Cai, Q. Zhang, X. Zhou, Y. Zhu, P. K. Shen and K. Zhang, ACS applied materials & interfaces, 2015, 7, 26512-26521.

78 W. Yang, Z. Gao, J. Ma, X. Zhang, J. Wang and J. Liu, Journal of Materials Chemistry A, 2014, 2, 1448-1457.
79 Y. Mo, Q. Ru, J. Chen, X. Song, L. Guo, S. Hu and S. Peng, Journal of Materials Chemistry A, 2015, 3, 19765-19773.
80 W. Zhang, X. Yan, X. Tong, J. Yang, L. Miao, Y. Sun and L. Peng, Materials Letters, 2015, 159, 313-316.
81 J. Wu, R. Mi, S. Li, P. Guo, J. Mei, H. Liu, W.-M. Lau and L.-M. Liu, RSC Advances, 2015, 5, 25304-25311.
82 M. Huang, F. Li, X. L. Zhao, D. Luo, X. Q. You, Y. X. Zhang and G. Li, Electrochimica Acta, 2015, 152, 172-177.
83 J.-J. Shim, Electrochimica Acta, 2015, 166, 302-309.
84 W. Ren, D. Guo, M. Zhuo, B. Guan, D. Zhang and Q. Li, RSC Advances, 2015, 5, 21881-21887.
85 J. Wang, Q. Zhang, X. Li, D. Xu, Z. Wang, H. Guo and K. Zhang, Nano Energy, 2014, 6, 19-26.
86 S. Wang, J. Pu, Y. Tong, Y. Cheng, Y. Gao and Z. Wang, Journal of Materials Chemistry A, 2014, 2, 5434-5440.
87 R. Zou, M. F. Yuen, Z. Zhang, J. Hu and W. Zhang, Journal of Materials Chemistry A, 2015, 3, 1717-1723.
88 L. Gao, X. Wang, Z. Xie, W. Song, L. Wang, X. Wu, F. Qu, D. Chen and G. Shen, Journal of Materials Chemistry A, 2013, 1, 7167-7173.
89 L. Gao, F. Qu and X. Wu, Journal of Materials Chemistry A, 2014, 2, 7367-7372.
90 H. Li, Z. Xia, J. Chen, L. Lei and J. Xing, Applied Catalysis B: Environmental, 2015, 168, 105-113.
91 Z. Ren, Y. Guo, G. Wrobel, D. A. Knecht, Z. Zhang, H. Gao and P.-X. Gao, Journal of Materials Chemistry, 2012, 22, 6862-6868.
92 R. D. Reitz, Combustion and Flame, 2013, 1, 1-8.
93 H. Garg, S. Mullick and V. K. Bhargava, Solar thermal energy storage, Springer Science & Business Media, 2012.
94 A. S. Arico, P. Bruce, B. Scrosati, J.-M. Tarascon and W. Van Schalkwijk, Nature materials, 2005, 4, 366-377.
95 Y. Liu and K. Xie, Science of Advanced Materials, 2014, 6, 863-874.
96 V. Tomašić and F. Jović, Applied Catalysis A: General, 2006, 311, 112-121.